

9th U. S. National Combustion Meeting
Organized by the Central States Section of the Combustion Institute
May 17-20, 2015
Cincinnati, Ohio

Enhancement of Premixed Methane-Air Flames by Halon 1301 Replacements

J.L. Pagliaro¹, G.T. Linteris², P.B. Sunderland¹, P.T. Baker³

¹*Dept. of Fire Protection Engineering, University of Maryland, College Park, MD 20742, USA*

²*Fire Research Division, National Institute of Standards and Technology, Gaithersburg, MD 20899, USA*

³*The Boeing Company, Seattle, WA 98124, USA*

Abstract: Apparent combustion enhancement by some halon replacement fire suppressants (proposed for use in aircraft cargo bays) has been observed in full-scale, constant-volume tests at the FAA. In order to explore the phenomena, laboratory-scale constant-volume combustion experiments were performed. The maximum explosion pressure and burning velocity were measured for methane-air flames with added CF₃Br (Halon 1301), C₆F₁₂O (Novec 1230), C₃H₂F₃Br (2-BTP), and C₂HF₅ (HFC-125). The explosion pressure, for initially stoichiometric flames, was increased mildly (up to 11% and 6%) with C₆F₁₂O and C₂HF₅ added at low concentrations, while at lean conditions ($\Phi=0.6$), it was increased about 50% for added C₆F₁₂O, C₃H₂F₃Br, or C₂HF₅, at agent volume fractions $X_a=0.02$, 0.03, and 0.06. The burning velocity for initially stoichiometric flames was always decreased with addition of any of the agents, whereas, for the lean conditions, it increased with added C₆F₁₂O or C₂HF₅ (32% and 14%, at $X_a=0.01$ and 0.03). Burning velocities at higher initial pressure (3 bar) and temperature (400 K) showed lower inhibition effectiveness (than at ambient conditions) for the stoichiometric flames, and larger enhancement for the lean flames (and the effect was due primarily to the temperature increase). CF₃Br did not increase the explosion pressure or burning velocity for any of the tested conditions. Equilibrium calculations were used to interpret the experiments. The present work is consistent with the FAA results and previous analysis of the full-scale tests.

Keywords: *Fire suppression, aircraft cargo bay fire protection, halon replacement, CF₃Br*

1. Introduction

Halon 1301 (CF₃Br) is an effective fire suppressant that has been banned for use in most applications by the Montreal Protocol. Additionally, the European Union is requiring replacement of CF₃Br in newly constructed aircraft by 2018 and in existing aircraft by 2040. As a result of the expected phase-out, three potential drop-in halon replacements were tested by the Federal Aviation Administration (FAA) for use in cargo bays; unfortunately, all of the agents failed the FAA Aerosol Can Test (FAA-ACT). The test simulates the explosion of an aerosol can caused by a fire in the cargo bay. In the FAA-ACT, air and suppressant are premixed in a simulated cargo bay compartment (a pressure vessel, 11.4 m³ in volume), in which a fast-acting valve releases the simulated can contents (a two-phase spray of alcohol, propane, and water) past a continuous high-voltage DC arc. In the absence of suppressant, the pressure rise in the chamber is about 2 bar. Through repeated tests at different agent volume fractions X_a , the inerting concentration of an agent is determined as the value of X_a required to prevent significant pressure rise. The standard also requires that an agent, when added at sub-inerting concentrations, cannot produce a higher pressure rise than the uninhibited case. All of the agents tested (C₆F₁₂O, Novec 1230, FK-5-1-12, CF₃CF₂C(=O)CF(CF₃)₂; C₃H₂F₃Br, 2-BTP,

$\text{CH}_2\text{CBrCF}_3$; and C_2HF_5 , CHF_2CF_3 , HFC-125), failed this element of the test, whereas CF_3Br did not [1, 2].

Experimental and numerical investigations of laboratory flames have described enhanced combustion with addition of halogenated suppressants, as outlined in ref. [3]. The phenomena include increased total heat release, widened lean flammability limits, decreased ignition delay, and increased pressure rise. Most of the early work documented the effects, but did not analyze the causes. In more recent work [3-9], numerical combustion simulations have been applied to gain insight using recently developed (or updated) kinetic mechanisms [10-13]. The studies have concluded that exothermic reaction of the fire suppressants adds energy to the constant volume system, increasing the overpressure. To obtain the observed pressure rise in the FAA-ACT, agent reaction is shown to occur under very fuel-lean equivalence ratios (Φ , based on the aerosol can fuel only), nearly corresponding to pure agent and air. Kinetic calculations have indicated that adding agents to fuel-lean flames can increase not only the energy release, but the rate of reaction as well. Nonetheless, no laboratory-scale experiments have been conducted to validate the explanations or to explore the combustion enhancement observed in the FAA tests for the new agents $\text{C}_6\text{F}_{12}\text{O}$ and $\text{C}_3\text{H}_2\text{F}_3\text{Br}$ (and experiments for C_2HF_5 are limited [14, 15]).

In the present work, the agents used in the FAA-ACT (CF_3Br , $\text{C}_6\text{F}_{12}\text{O}$, $\text{C}_3\text{H}_2\text{F}_3\text{Br}$, and C_2HF_5) are added at various sub-inerting concentrations to stoichiometric and lean methane-air flames in a laboratory-scale constant-volume chamber to determine their influence on the maximum pressure rise and burning velocity. The effects of compressive heating on the burning velocity are also determined. The goals of the present work are to test the concepts developed via numerical simulations and analysis of the FAA tests [3, 4, 7] and to reproduce the phenomena observed in the complex full-scale FAA experiments.

2. Experimental

2.1. Apparatus and Procedure

Experiments are performed in a spherical, constant-volume apparatus with an inner diameter of 15.24 cm, volume of 1.85 L, and wall thickness of 2.54 cm (similar to previous designs [16-18]). Sensors include an absolute pressure gage, a dynamic pressure sensor, and a thermocouple, so that the experiment can provide directly the temperature rise and explosion pressure. Further processing of the pressure data yields the instantaneous laminar burning velocity (1-D spherical) as a function of pressure and temperature.

The experimental method is similar to past work [19], therefore only a brief description is provided. We prepare test mixtures in the chamber using the partial pressure method, first with injection of liquid followed by gaseous reactants. The partial pressure of each mixture component is determined with an absolute pressure transducer (Omega, PX811; claimed accuracy of 0.1% of reading) that is periodically calibrated against a Baratron 627D (claimed accuracy of 0.12%) and a Wallace & Tiernan 1500 pressure gage (claimed accuracy of 0.066%). Liquid suppressants ($\text{C}_6\text{F}_{12}\text{O}$ and $\text{C}_3\text{H}_2\text{F}_3\text{Br}$) are injected using a syringe via a gas-tight septum (which is separated from the chamber by a ball valve to ensure leak-free operation during the explosion event). The sample gases are CH_4 (Matheson Tri-Gas, 99.97% purity), CF_3Br (Great Lakes Chemical Corp., 99.6% purity), $\text{C}_6\text{F}_{12}\text{O}$ (3M, > 99% purity), $\text{C}_3\text{H}_2\text{F}_3\text{Br}$ (American Pacific Corp., > 99% purity), and C_2HF_5 (Allied Signal Chemicals, 99.5% purity). The air is house compressed air (filtered and dried) that is additionally conditioned with a 0.01 μm filter, carbon filter, and a desiccant bed to remove small aerosols, organic vapors, and water vapor before use.

The relative humidity of the air is less than 2% for all tests. The reactant mixture is given 10 minutes to settle before combustion is initiated using a capacitive discharge ignition system (described in further detail in ref. [19]) that provides a controlled spark with an estimated energy range of 0.05-500 mJ. Two tungsten electrodes form an adjustable gap (typically 2 mm) in the center of the chamber, and thin electrodes (diameter of 0.4 mm) ensure minimal heat loss from the flame. The explosion pressure is recorded at 4000 Hz using a dynamic pressure sensor with a claimed accuracy of 0.1% of reading.

2.2. Burning Velocity from the Pressure Trace

Laminar burning velocity is determined from the pressure trace using a thermodynamic model that is summarized briefly below, with more details available in ref. [19]. The contents of the chamber are divided into burned and unburned zones separated by an infinitely thin flame sheet. Flame propagation is assumed to be spherical and smooth, creating a spatially uniform pressure rise. All gases are considered ideal and semi-perfect (variable specific heats), with the unburned gas frozen at its initial composition, and the burned gas composition represented by thermodynamic equilibrium products of a constant volume, constant energy process (calculated using CEA2 [20]). Both zones are adiabatic, and the unburned gas is compressed isentropically as the flame expands. With these assumptions, the laminar burning velocity S_L is expressed in terms of known variables in Eq. 1 (more details in refs. [16, 21]),

$$S_L = R/3[1 - (1 - x_b)(P_0/P)^{1/\gamma_u}]^{-2/3}(P_0/P)^{1/\gamma_u}(dx_b/dt) \quad (1)$$

where R the chamber radius, x_b the mass fraction of burned gas, P the instantaneous pressure, P_0 the initial pressure, and γ_u the specific heat ratio of the unburned gases. The thermodynamic model relates the mass fraction of burned gas x_b to the instantaneous pressure P . The mass and energy conservation equations are solved simultaneously for the chamber contents (burned and unburned gases), using Eqs. 2 and 3.

$$\frac{V}{M} = \int_0^{x_b} v_b dx + \int_{x_b}^1 v_u dx \quad (2)$$

$$\frac{E}{M} = \int_0^{x_b} e_b dx + \int_{x_b}^1 e_u dx \quad (3)$$

where V is the chamber volume and E and M are internal energy and mass of the initial contents, e and v are the internal energy and specific volume of the gas, and the subscripts b and u refer to the burned and unburned gas.

Polynomial coefficients (for the major reactant and product species) are taken from GRI-mech 3.0 [22] (CH_4 , O_2 , N_2 , CO_2 , H_2O , CO , NO , OH , H_2 , and O), the NIST HFC mechanism [10] ($\text{C}_6\text{F}_{12}\text{O}$, C_2HF_5 , F , HF , CF_4 , and CF_2O), and Babushok et al. [11] (CF_3Br , $\text{C}_3\text{H}_2\text{F}_3\text{Br}$, Br , HBr , and Br_2) to describe the thermodynamic properties of the burned and unburned gas. The instantaneous unburned gas temperature is related to the pressure through isentropic compression. The unburned gas properties v_u and e_u in Eqs. 2 and 3 are calculated at each pressure increment from the unburned gas composition and temperature T_u , reducing the model to two equations and two unknowns (T_b and x_b). The remaining unknowns in the conservation equations (v_b , e_b , and x_b) are found using a non-linear optimization routine that iterates on T_b (v_b and e_b are functions of temperature) and x_b at each pressure increment, until the proper values of T_b and x_b are obtained. Once $x_b(P)$ is known, the burning velocity $S_L(P, T_u)$ is determined over the experimental range of pressure and temperature using Eq. 1.

2.3. Data Reduction

When the flame radius r_f is small, the flame propagation rate can be affected by flame stretch and by excess energy deposited during the ignition process; whereas when r_f is large, flame propagation can be affected by heat loss to the chamber walls. Therefore, only a portion of the pressure data from each experiment is used (typically the central 75%) to calculate burning velocity in the present study. As expressed in Eq. 4, outwardly propagating spherical flames are subject to stretch rates that are inversely proportional to r_f [23],

$$\kappa = \frac{2}{r_f} \frac{dr_f}{dt} \quad (4)$$

where κ is the stretch rate and dr_f/dt is the flame front velocity. The effects of stretch and ignition are reduced by neglecting data when the flame radius r_f is less than 50% of the chamber radius R , as proposed by Elia [24]. Additionally, only data up to dP/dt_{max} (i.e., the inflection point on the $P(t)$ curve) are considered, eliminating data affected by heat loss to the walls.

The pressure data from an individual test are used to determine the burning velocity at each combination of unburned gas pressure and temperature occurring during the test. Tests are performed at $T_0=296\pm 2$ K, and at $P_0=0.868$ bar, 1 bar, and 1.13 bar to increase the number of combinations. The results of multiple tests (repeated twice for each initial pressure) are fit to Eq. 5 [33] to decouple the influences of pressure and temperature on S_L ,

$$S_L = S_{L,0} \left(\frac{T}{T_0}\right)^\alpha \left(\frac{P}{P_0}\right)^\beta \quad (5)$$

where S_L is the laminar burning velocity, P_0 is the initial pressure, T_0 is the initial temperature, $S_{L,0}$ is the laminar burning velocity at the initial conditions; α , β , and $S_{L,0}$ are the fitting parameters. In discussions following, S_L is presented at ambient conditions ($P=1$ bar; $T=298$ K) and elevated conditions ($P=3$ bar; $T=400$ K) as obtained from Eq. 5. Note that the presented results are interpolations, or small extrapolations, from the experimental data. As determined previously [19], the relative uncertainty in reported burning velocities is 6%.

Spherical flame propagation is a critical condition for reliable calculation of S_L from the pressure trace. For slower flames (i.e., inhibited flames) with long propagation times, buoyant forces are not negligible; therefore, to reduce experimental inaccuracies, only flame speeds that are greater than 6 cm/s are reported, as recommended by ref. [18]. Cellular instabilities, which also invalidate the spherical flame assumption, are monitored through inspection of the S_L data of individual test runs. The onset of cellular instabilities is detected via a distinct increase in the burning velocity [25], which did not occur in any of the data contained in the present study.

3. Results and Discussion

3.1. Peak Pressure Rise

The maximum pressure rise of methane-air explosions in a closed vessel was determined with addition of CF_3Br , $\text{C}_6\text{F}_{12}\text{O}$, $\text{C}_3\text{H}_2\text{F}_3\text{Br}$, and C_2HF_5 ($T_0=296\pm 2$ K, $P_0=1$ bar). Agents were added to stoichiometric flames and lean flames with a fuel-air equivalence ratio Φ of 0.6 (Φ based on uninhibited mixtures, i.e., when an agent is added, proportional quantities of methane and air are displaced). Figure 1 shows the results for the stoichiometric and lean systems. The peak pressure rise ΔP_{max} from experiments is shown, along with the calculated equilibrium ΔP_{max} and adiabatic temperature T_{ad} (calculated using CEA2, for a constant internal energy, constant volume system). The line style (and color) denoting the results for each agent are defined via the

experimental curves, and the assignment is preserved for the two sets of equilibrium curves. For reference, the uninhibited stoichiometric system has $T_{ad}=2599$ K and $\Delta P_{max}=7.94$ bar at equilibrium. Adding CF_3Br decreases T_{ad} , whereas adding any of the other agents slightly increases T_{ad} (≈ 2612 K) at low X_a , and then decreases it as X_a increases, with the larger inhibitor molecules decreasing T_{ad} more. The observed increases in T_{ad} are comparable to the increase that occurs from stoichiometric to slightly rich conditions in methane-air systems (peak $T_{ad}=2615$ K at $\Phi=1.07$).

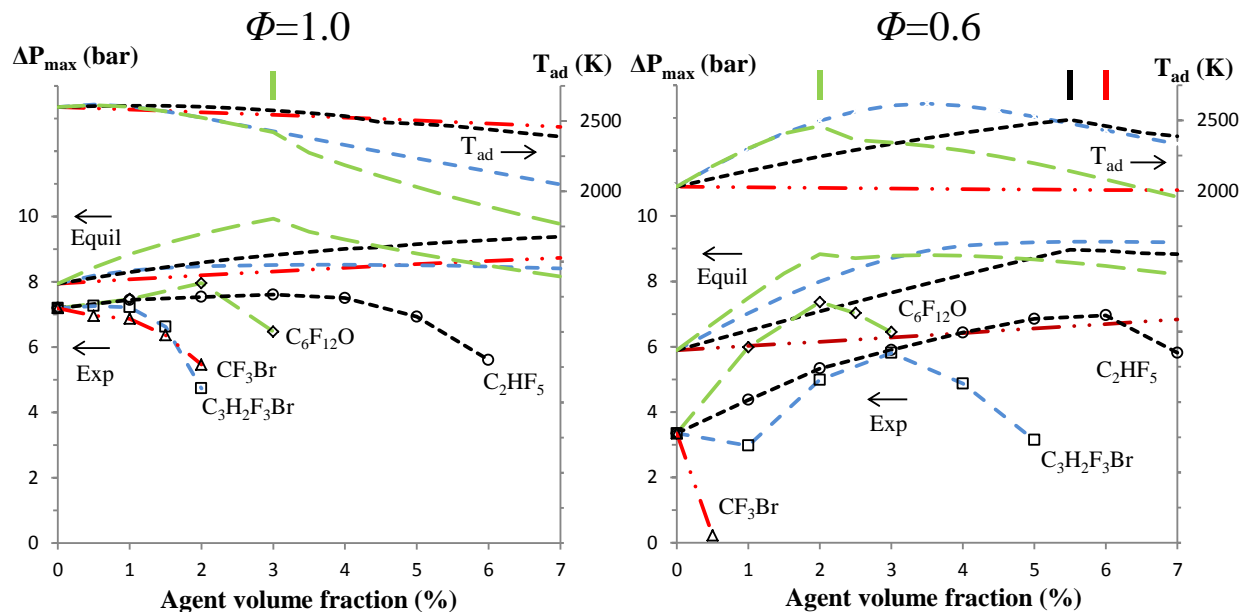


Figure 1: Pressure rise (left scale) and adiabatic temperature (right scale) in constant-volume combustion sphere with agents added to methane-air flames ($\Phi=1.0$, left frame, $\Phi=0.6$, right frame). Lines: equilibrium calculations; lines with symbols: experiments.

For the stoichiometric case (left frame in Figure 1), the equilibrium pressure (lines with no symbols) increases with addition of each agent, including CF_3Br , up to a certain value of X_a , then drops for higher X_a . The value of X_a controlling this behavior is related to the halogen X to hydrogen H ratio $[X]/[H]$ in the premixed gases, which is equal to unity for CF_3Br , $C_6F_{12}O$, $C_3H_2F_3Br$, and C_2HF_5 at $X_a=0.09$, 0.03 , 0.16 , and 0.09 (as indicated by the vertical lines at the top of the figure). Since X_a for $[X]/[H]=1$ is off the figure when adding CF_3Br , $C_3H_2F_3Br$, and C_2HF_5 to the stoichiometric case, the equilibrium ΔP_{max} increases continuously. The increase in ΔP_{max} is caused by the increase in the number of moles of products, which overrides the lower values of T_{ad} with agent addition. For X_a above $[X]/[H]=1$, the equilibrium products change (formation of COF_2 rather than HF , as a fate for F), so the number of moles of product decreases, reducing ΔP_{max} . As with T_{ad} , the equilibrium value of ΔP_{max} is higher for larger molecules (at least at low values of X_a), but they reach $[X]/[H]=1$ at different values of X_a , which dominates their behavior. With agent added to these stoichiometric flames, $C_6F_{12}O$, $C_3H_2F_3Br$, and C_2HF_5 , have a maximum equilibrium pressures rise 2 bar, 1.5 bar, and 0.6 bar higher than with no agent, occurring at $X_a=0.03$, 0.07 , and 0.04 . Note that the equilibrium ΔP_{max} is relatively insensitive to X_a for $C_3H_2F_3Br$, and that calculations show an increase in ΔP_{max} even for addition of CF_3Br .

As shown in Figure 1 (again for $\Phi=1$), the experimentally determined ΔP_{max} of all agents is less than the equilibrium value. For example, the uninhibited stoichiometric methane-air

system has an experimental $\Delta P_{max}=7.2$ bar, which is close to $\Delta P_{max}=7.3$ bar measured by ref. [26] and about 9% lower than the equilibrium value. To some extent, the experimental values of ΔP_{max} with added agent follow the trends in the equilibrium values, although the experimental ΔP_{max} rises more slowly than the equilibrium value, before eventually dropping rapidly. This can be caused by flame quenching (from heat losses at the wall [27] or from buoyancy [28]), by radiative heat loss, and (for these initially stoichiometric flames) by kinetic quenching of the flame reactions. While it is possible to define an extent of reaction λ based on the ratio of measured to equilibrium ΔP_{max} [27], this is of limited value in the present work since the effects interact: slower burning velocities (with inhibitor) allow more time for buoyancy to act, and buoyancy-induced quenching lowers the temperature (and hence the overall reaction rate), which can also affect the kinetic inhibition. Also, the effects are likely to depend upon the size of the sphere and degree of turbulence [29] (which are different in the FAA-ACT test). Note that while equilibrium calculations predict enhanced pressure rise with CF_3Br and $\text{C}_3\text{H}_2\text{F}_3\text{Br}$, both have none, and have much reduced pressure rise as X_a increases (likely due to kinetic inhibition by the bromine [13]). For addition to stoichiometric flames, $\text{C}_6\text{F}_{12}\text{O}$ and C_2HF_5 increase the experimental ΔP_{max} by 11% and 6%, at $X_a=0.02$ and $X_a=0.03$.

Results for lean methane-air mixtures ($\Phi=0.6$) are shown in the right frame of Figure 1. For reference, the equilibrium adiabatic temperature and pressure rise for an uninhibited methane-air mixture at $\Phi=0.6$ are 2031 K and 5.89 bar. With agent added to these lean flames, $\text{C}_6\text{F}_{12}\text{O}$, $\text{C}_3\text{H}_2\text{F}_3\text{Br}$, and C_2HF_5 , have peak T_{ad} which are 331 K, 589 K, and 473 K higher than the uninhibited case, occurring at $X_a=0.025$, 0.035, and 0.055 (for $\text{C}_3\text{H}_2\text{F}_3\text{Br}$, the peak value of T_{ad} is 20 K higher than that of the uninhibited stoichiometric methane-air flame, while for C_2HF_5 and $\text{C}_6\text{F}_{12}\text{O}$ it's about 100 K and 140 K lower). The increase in T_{ad} is due to the higher enthalpy of formation of the reactant mixture, and the stable product species (e.g., CO_2 , HF , etc.); that is, with regard to the thermodynamics, the agents have fuel-like properties. In contrast, T_{ad} decreases by roughly 5 K for every 1% of added CF_3Br . For the pressure rise, the equilibrium results again show an increase in ΔP_{max} with addition of each agent, reaching a peak near the X_a for which $[\text{X}]/[\text{H}]=1$ (at $X_a\approx 0.06$, 0.02, 0.11, and 0.055 for CF_3Br , $\text{C}_6\text{F}_{12}\text{O}$, $\text{C}_3\text{H}_2\text{F}_3\text{Br}$, and C_2HF_5). For $\Phi=0.6$, however, both the relative and absolute pressure rise are much bigger than for $\Phi=1$, with equilibrium ΔP_{max} increasing by nearly 50% with addition of $\text{C}_6\text{F}_{12}\text{O}$, $\text{C}_3\text{H}_2\text{F}_3\text{Br}$, or C_2HF_5 . In the experiments, the pressure rise was again always lower than the equilibrium value (i.e., $\lambda < 1$). For example, for $X_a=0$, ΔP_{max} was 3.35 bar, or 43% lower than the equilibrium value, or $\lambda=0.57$, which is much lower than the case of $\Phi=1$ and $X_a=0$, for which $\lambda=0.91$ (as discussed previously [28], slower flames are more strongly influenced by buoyancy-induced quenching). With addition of the agents, however, the behavior for $\Phi=0.6$ is different from that for $\Phi=1$. For the lean flames, λ often increases as X_a increases, as compared to the $\Phi=1$ case for which λ decreases. With regard to the peak experimental pressure rise, addition of $\text{C}_6\text{F}_{12}\text{O}$, $\text{C}_3\text{H}_2\text{F}_3\text{Br}$, or C_2HF_5 yielded a ΔP_{max} of 7.36 bar, 5.81 bar, or 6.96 bar, at X_a of 0.02, 0.03, or 0.06. These values are 2.2, 1.7, and 2.1 times the ΔP_{max} for the uninhibited system (3.35 bar). In contrast, addition of CF_3Br at $X_a=0.005$ extinguished the flame just after ignition, yielding $\Delta P_{max}=0.22$ bar.

The results for the explosion pressure in the 1.85 L chamber (for $\Phi=0.6$) clearly illustrate the combustion enhancement of the type observed in the FAA-ACT [1], whereas results for $\Phi=1$ do not adequately duplicate the behavior. Hence, reduced-scale explosion vessels, used to evaluate lean fuel-air systems, are a valuable tool for understanding the FAA-ACT results; for example, the measurements of ΔP_{max} highlight the increased heat release occurring with addition

of the halon replacements to the lean system. More than just the higher explosion pressure with added agent, however, the higher extent of reaction with added agent (in the $\Phi=0.6$ case) implies a higher burning velocity with agent addition to the lean flames. To more clearly investigate this possibility, the burning velocity is calculated from the pressure rise data (as described above) to more clearly delineate the effect of the agents on the overall reactivity of the system.

3.2. Laminar Burning Velocity

The laminar burning velocity was measured for the stoichiometric ($\Phi=1$) and lean ($\Phi=0.6$) methane-air flames with added agents. Initial conditions were $T_0=296\pm 2$ K, and $P_0=0.868$ bar, 1 bar, and 1.13 bar, (to provide more data for the curve fit). For each agent, tests were conducted up to values of X_a for which $S_L\approx 6$ cm/s (since buoyant distortion has been found to be minimal for $S_L\geq 6$ cm/s). For each value of Φ and X_a , tests were conducted at the three values of P_0 , providing the fitting parameters $S_{L,0}$, α , and β in Eq. 5 above. The burning velocity of the inhibited flames for each of the agents is presented in Figure 2 ($\Phi=1$, left frame; $\Phi=0.6$, right frame) as the normalized burning velocity (for a given Φ and agent, S_L at X_a is divided by S_L with $X_a=0$). For reference, uninhibited burning velocities are 35.8, 8.3, 44.5, and 10.0 cm/s for $\Phi=1.0$ and 0.6 at ambient conditions (298 K, 1 bar) and compressed conditions (400 K, 3 bar), respectively. Results for each agent are illustrated with different style symbols; closed and open symbols represent data at standard and compressed conditions.

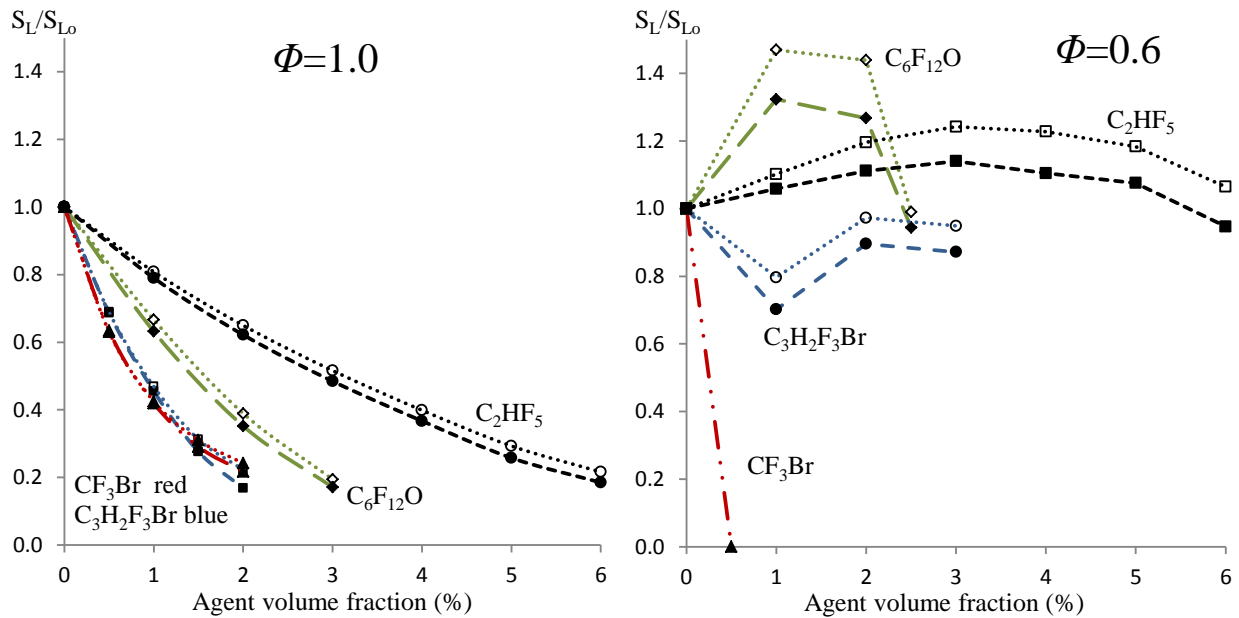


Figure 2: Normalized burning velocity with agents added to CH_4 -air flames ($\Phi=1.0$, left frame; $\Phi=0.6$, right frame). Dashed lines: $P_0=1$ bar, $T_0=298$ K; dotted lines: $P_0=3$ bar, $T_0=400$ K.

As Figure 2 shows, for stoichiometric flames, adding each agent reduces S_L at all values of X_a , with a decreasing marginal effectiveness at higher X_a , as has been discussed previously [30]. On a molar basis, $\text{C}_6\text{F}_{12}\text{O}$ requires 1/2 as much as C_2HF_5 for a comparable reduction in S_L , and $\text{C}_3\text{H}_2\text{F}_3\text{Br}$, about 1/3 as much. The performance of $\text{C}_3\text{H}_2\text{F}_3\text{Br}$ and CF_3Br are roughly equivalent (on a molar basis), although CF_3Br is slightly more effective for $X_a < 0.01$, and $\text{C}_3\text{H}_2\text{F}_3\text{Br}$ for $X_a > 0.01$. This is consistent with cup burner results (heptane) [31, 32] for which $\text{C}_3\text{H}_2\text{F}_3\text{Br}$ was found to have a lower minimum extinguishing concentration (2.6%) than CF_3Br

(2.9%), and $C_6F_{12}O$ required roughly 50 % more than CF_3Br (4.5%). Comparison of the results at ambient ($T_0=298$ K, $P_0=1$ bar) vs. compressed ($T_0=400$ K, $P_0=3$ bar) conditions shows that while the compressed flames have an uninhibited value of S_L about 14% higher, the reduction in normalized S_L with added agents is about 2% less for the compressed flames than for the ambient flames at low values of X_a , and 4% less at high values of X_a . This can be compared to flame inhibition by CO_2 , for which the calculated normalized reduction in S_L at $T_0=353$ K as compared to $T_0=298$ K was 8%, 4%, and 0.3% lower at $X_a=0.03$, 0.07, and 0.15 [33]. That is, for these initially stoichiometric flames, these changes in the unburned gas conditions do not appear to significantly affect the inhibition kinetics of these agents.

For the lean ($\Phi=0.6$) flames, the effects of added agents on S_L are different than at $\Phi=1$. For $T_0=298$ K, $C_6F_{12}O$ and C_2HF_5 increase S_L by 32% and 13% at $X_a=0.01$ and 0.03. That is, with $C_6F_{12}O$ or C_2HF_5 added to lean flames of methane–air, the mixture becomes more reactive, with significantly increased burning velocity: S_L is increased for all values of X_a up to about 0.025 for $C_6F_{12}O$, and 0.065 for C_2HF_5 . In contrast, with CF_3Br addition to the lean flame (at $X_a=0.005$), the mixture was not flammable when subject to the highest available ignition energy. (The dashed line in the right frame of Figure 2 is included to illustrate the inerting nature of CF_3Br at $X_a=0.005$ and is not intended to provide S_L values between those measured at $X_a=0$ and $X_a=0.005$.) The results for $C_3H_2F_3Br$ are intermediate between those of CF_3Br and the other agents: for $X_a=0.01$, S_L decreases by 30%, but as X_a increases, S_L increases so that at $X_a=0.02$ and 0.03, S_L is only about 10% lower than the uninhibited flames. Note that with $C_3H_2F_3Br$ addition to the lean flame, the measured S_L is never higher than with no agent. Apparently, the gas-phase catalytic radical recombination cycles of brominated species have a larger inhibition effect in the present flames than the promotion effect of the agent due to the increased temperature [13]. With $C_6F_{12}O$ addition, S_L drops rapidly above $X_a=0.02$, and with C_2HF_5 addition, it drops slowly above $X_a=0.03$. At the compressed condition, the peak enhancement in S_L with addition of $C_6F_{12}O$ and C_2HF_5 is larger by 47% and 24%, while the decrease in S_L with $C_3H_2F_3Br$ addition is less. (Note that from the fitting parameters of Eq. 5, the effect of compression is primarily caused by higher temperature, not pressure, which has a small effect for the present range of variation in T and P .)

The present results illustrate that when added to lean premixed methane-air flames at low concentrations, the agents $C_6F_{12}O$ and C_2HF_5 actually increase the burning velocity, and for $C_3H_2F_3Br$ addition, the burning velocity is reduced slightly (about 10% at $X_a=0.02$ or 0.03). These results, together with the measured higher explosion pressures in the presence of these agents, are consistent with the higher overpressures in the FAA-ACT. Under lean conditions in the FAA-ACT, exothermic reaction of the agent creates higher overpressure than with no agent, and apparently the reaction rate is not sufficiently slowed (or is actually increased) with agent addition, so as to reduce the overpressure. In contrast, addition of CF_3Br both reduces the reaction rate for all stoichiometries, and causes no increase in the explosion pressure. These principles were predicted in numerical simulations, but the present results are experimental verification of the principles previously outlined [3, 4, 7, 9], and the first to show increased flame speed of lean flames with added halon replacements.

4. Conclusions

Several potential halon replacements, for use in cargo-bay fire suppression, failed a mandated FAA performance test. To help understand their behavior, experiments were performed in a constant-volume combustion device (premixed CH_4 -air system) to measure the

peak pressure rise and burning velocity resulting from addition of the agents (CF_3Br , $\text{C}_6\text{F}_{12}\text{O}$, $\text{C}_3\text{H}_2\text{F}_3\text{Br}$, and C_2HF_5).

The influence of the agents on explosion pressure varied with agent type and concentration, as well as the initial stoichiometry of the methane-air mixture. For stoichiometric flames, addition of CF_3Br or $\text{C}_3\text{H}_2\text{F}_3\text{Br}$ reduced the peak pressure rise at all agent loadings; while $\text{C}_6\text{F}_{12}\text{O}$ and C_2HF_5 increased ΔP_{max} slightly at low loadings ($X_a \leq 0.02$ and 0.03), and reduced it at higher X_a . In lean ($\Phi=0.6$) flames, however, addition of $\text{C}_6\text{F}_{12}\text{O}$, $\text{C}_3\text{H}_2\text{F}_3\text{Br}$, and C_2HF_5 all increased the pressure rise, with a peak pressure rise of about a factor of two above the uninhibited case, and occurring at agent loadings of 2% to 6%, depending upon the agent. In contrast, CF_3Br caused no increase in the ΔP_{max} at any condition.

All agents were found to reduce burning velocity of stoichiometric methane-air flames at the concentrations tested. CF_3Br and $\text{C}_3\text{H}_2\text{F}_3\text{Br}$ caused similar flame speed reductions (about 55% at $X_a=0.01$), with CF_3Br slightly more effective at $X_a=0.01$ and below, and $\text{C}_3\text{H}_2\text{F}_3\text{Br}$ more effective above. $\text{C}_6\text{F}_{12}\text{O}$ and C_2HF_5 were about 2/3 and 1/3 as effective as CF_3Br at reducing the burning velocity of stoichiometric flames. For lean ($\Phi=0.6$) methane-air flames at ambient initial temperature and pressure, addition of $\text{C}_6\text{F}_{12}\text{O}$ and C_2HF_5 at sub-inerting concentrations increased the burning velocity by 32% and 13%. That is, when added to lean flames, not only do they increase the explosion pressure, but they can also enhance the reactivity. Addition of $\text{C}_3\text{H}_2\text{F}_3\text{Br}$ slightly decreased the burning velocity (for $X_a \leq 0.03$), while addition of CF_3Br (at $X_a=0.005$) inerted the mixture.

The data also provided burning velocities at compressed conditions ($P_0=3$ bar, $T_0=400$ K), for which agent addition to stoichiometric methane-air mixtures reduced the burning velocities slightly less than at ambient conditions ($P_0=1$ bar, $T_0=298$ K). For the lean ($\Phi=0.6$) mixtures, addition of $\text{C}_6\text{F}_{12}\text{O}$ or C_2HF_5 increased the burning velocity (over uninhibited values) significantly (≈ 25 -50%) more than for the ambient conditions. Similarly, the reduction in the burning velocity with $\text{C}_3\text{H}_2\text{F}_3\text{Br}$ addition was reduced at the compressed condition. The experimental data indicate that the stronger enhancement at compressed conditions is due almost entirely to the higher temperature, not pressure.

In practice, when used to suppress fires, clean agents are typically added at concentrations high enough to extinguish the flames. In the present tests (and as apparently occurs in the FAA Aerosol Can test), however, when some halon replacements are added to lean mixtures (in closed vessels) at sub-inerting concentrations, they can enhance both the pressure rise and rate of reaction.

5. Acknowledgements

This research was funded by the Boeing Company and a NIST-ARRA grant.

6. References

1. J. Reinhardt, *Behavior of Bromotrifluoropropene and Pentafluoroethane When Subjected to a Simulated Aerosol Can Explosion*, DOT/FAA/ARTN04/4, Federal Aviation Administration, 2004.
2. J. Reinhardt, *Aircraft Cargo MPS Test of FK-5-1-12*, International Aircraft Systems Fire Protection Working Group, Federal Aviation Administration, October 25–26, 2006.
3. G.T. Linteris, D.R. Burgess, F. Takahashi, V.R. Katta, H.K. Chelliah, and O. Meier, *Combust. Flame* 159 (2012) 1016-1025.
4. G. Linteris, F. Takahashi, V. Katta, H. Chelliah, and O. Meier, *Int. Assoc. Fire Saf. Sci.* (2011) 1-14.
5. V.I. Babushok, G.T. Linteris, and O.C. Meier, *Combust. Flame* 159 (2012) 3569-3575.

Sub Topic: Fire

6. F. Takahashi, V.R. Katta, G.T. Linteris, and O.C. Meier, Proc. Combust. Inst. 34 (2013) 2707-2717.
7. G.T. Linteris, V.I. Babushok, P.B. Sunderland, F. Takahashi, V.R. Katta, and O. Meier, Proc. Combust. Inst. 34 (2013) 2683-2690.
8. F. Takahashi, V.R. Katta, G.T. Linteris, V. Babushok, and P.T. Baker, Proc. Combust. Inst. (2014)
9. G.T. Linteris, V.I. Babushok, D.R. Burgess, J.A. Manion, F. Takahashi, V. Katta, and P.T. Baker, Proc. Combust. Inst. 35 (2014)
10. D. Burgess, M. Zachariah, and P. Westmoreland, Prog. in Energy and Combust. Sci. 21 (1996) 453-529.
11. V. Babushok, T. Noto, D.R.F. Burgess, A. Hamins, and W. Tsang, Combust. Flame 107 (1996) 351-367.
12. V.I. Babushok, G.T. Linteris, O.C. Meier, and J.L. Pagliaro, Combust. Sci. Technol. 186 (2014) 792-814.
13. V. Babushok, D.R. Burgess JR., G.T. Linteris, and O. Meier, Combust. Flame, <http://dx.doi.org/10.1016/j.combustflame.2014.10.002> (2014)
14. Y.N. Shebeko, V.V. Azatyan, I.A. Bolodian, V.Y. Navzenya, S.N. Kopylov, D.Y. Shebeko, and E.D. Zamishevski, Combust. Flame 121 (2000) 542-547.
15. G.T. Linteris, D.R. Burgess, V. Babushok, M. Zachariah, W. Tsang, and P. Westmoreland, Combust. Flame 113 (1998) 164-180.
16. M. Metghalchi and J.C. Keck, Combust. Flame 38 (1980) 143-154.
17. R. Stone, A. Clarke, and P. Beckwith, Combust. Flame 114 (1998) 546-555.
18. K. Takizawa, A. Takahashi, K. Tokuhashi, S. Kondo, and A. Sekiya, Combust. Flame 141 (2005) 298-307.
19. J.L. Pagliaro, G.T. Linteris, P.B. Sunderland, and P.T. Baker, Combust. Flame 162 (2015) 41-49.
20. S. Gordon and B.J. McBride, *Computer program for calculation of complex chemical equilibrium compositions and applications*, N.R.P. 1311, Editor. 1996, NASA Glenn Research Center: Cleveland, OH.
21. P.G. Hill and J. Hung, Combust. Sci. Technol. 60 (1988) 7-30.
22. G.P. Smith, D.M. Golden, M. Frenklach, N.W. Moriarty, B. Eiteneer, C. Mikhail Goldenberg, T. Bowman, R.K. Hanson, S. Song, J. William C. Gardiner, V.V. Lissianski, and Z. Qin. http://www.me.berkeley.edu/gri_mech/.
23. F.A. Williams. *AGARD Conference Proceeding*. 1975
24. M. Elia, M. Ulinski, and M. Metghalchi, J Eng for Gas Turbines and Power 123 (2001) 190.
25. K. Saeed and C.R. Stone, Combust. Flame 139 (2004) 152-166.
26. D. Razus, C. Movileanu, V. Brinzea, and D. Oancea, J Hazard Mater 135 (2006) 58-65.
27. K.L. Cashdollar, I.A. Zlochower, G.M. Green, R.A. Thomas, and M. Hertzberg, Journal of Loss Prevention in the Process Industries 13 (2000) 327-340.
28. A.E. Dahoe and L.P.H. de Goey, J Loss Prevent Proc 16 (2003) 457-478.
29. G.F.P. Harris, Combust. Flame 11 (1967) 17-25.
30. T. Noto, V. Babushok, A. Hamins, and W. Tsang, Combust. Flame 112 (1998) 147-160.
31. T.A. Moore, C.A. Weitz, and R.E. Tapscott. *Papers from 1991-2006 Halon Options Technical Working Conferences, NIST SP 984-4*. 2001.551-564.
32. B.P. Carnazza, J.G. Owens, P.E. Rivers, and J.S. Schmeer. *Papers from 1991-2006 Halon Options Technical Working Conferences, NIST SP 984-4*.
33. G.T. Linteris, M.D. Rumminger, V. Babushok, and W. Tsang, Proc. Combust. Inst. 28 (2000) 2965-2972.